



# ACOUSTIC RESONANCE IN THE COMBUSTION CONDUITS OF A STEAM LOCOMOTIVE

S. ZIADA\* AND A. OENGÖREN

*Sulzer Innotec Limited, CH-8401, Winterthur, Switzerland*

AND

H. H. VOGEL

*Swiss Locomotive and Machine Works, Winterthur, Switzerland*

*(Received 11 November 1996 and in revised form 1 December 1997)*

The sound emission of a modern, oil-fired steam rack locomotive increased sharply when the locomotive speed exceeded the design value of 12 km/h. The results of pressure and noise measurements, together with an acoustical model of the combustion conduits, indicated that the acoustic resonance modes of the combustion conduits are excited by the pressure pulsations generated by the exhaust from the steam cylinders at multiples of the piston frequency. Additionally, when the acoustic resonance is initiated, the resulting pulsations trigger the flame instability of the oil burners which, in turn enhances the resonance. By means of the acoustical model, a Helmholtz resonator has been designed and optimized to reduce the acoustic response such that it does not excite the flame instability. A second set of measurements, after installing the resonator, has shown a reduction in the noise level by an amount exceeding 21 dBA. The paper focuses upon the identification of the excitation source and the implementation of the counter-measure, which are of interest to other applications involving combustion oscillations.

©1998 Academic Press

## 1. INTRODUCTION

THIS PAPER DEALS with a noise and vibration problem which appeared when the speed of a steam rack locomotive was increased beyond the maximum design value. The locomotive is designed to climb steep gradients in tourist areas, and therefore a relatively low maximum speed was targeted: about 10–12 km/h. However, peak speed values of 14 km/h cannot be excluded in actual operation. During the trial tests at this higher speed, loud noise and vibration were produced. The excitation mechanism causing this problem and means of its alleviation are described in this paper.

After a brief description of the locomotive geometry, the results of tests carried out on the original geometry are presented. The acoustical response of the system is then modelled by means of the acoustic-electrical circuits analogy (Kinsler *et al.* 1982). Thereafter, the effect of installing a Helmholtz resonator is studied with the aid of the electrical model. Finally, the test results of the locomotive with and without the Helmholtz resonator are compared.

---

\*Present address: Department of Mechanical Engineering, McMaster University, Hamilton, Ont. L8S 4L7, Canada.

## 2. LOCOMOTIVE GEOMETRY, OPERATION AND LOCATIONS OF MEASUREMENT

The geometry of the steam locomotive is shown in Figure 1. The main components of the combustion side are five oil burners (18)† and air inlets, a combustion chamber (1), a tube (5) and flue (6) section with the flues housing the superheater pipe loops (6), an exhaust chamber (15) and a chimney (14). The tube and flue section is referred to hereafter as the heat exchanger flue. Superheated steam (17) is used to atomize the fuel oil. The superheater loop is not shown in Figure 1. The locomotive is driven by two, double-acting steam cylinders (23) working on a crankshaft (27) with cranks set at 90° to each other.

A piston valve (30) controls the inlet and exhaust timing of the steam to and from both sides of each cylinder. Each piston valve is driven by a linkage which derives two motions from the crankshaft, one in phase with the piston taken from the cross-head (25), the other at 90° to the piston derived from a separate crank on the crankshaft. The stroke of the latter motion can be varied in amplitude and sign by means of the radius link (28) by the driver of the locomotive, allowing him to choose the rate of expansion of the steam in the cylinder, and thus the tractive effort and the running direction. Both motions are combined at the combination lever (29), which finally drives the valve itself.

The exhaust steam of both sides of the two cylinders is ducted into a Venturi blast nozzle (12), which injects into the mixing chamber (13), where an impulse exchange between the high-impulse exhaust steam and the slow combustion gas takes place, thus sucking the combustion gas through the system. The kinetic energy of the steam-gas mixture is finally recuperated in the diffuser (14).

Four evenly spaced steam pulses per crankshaft revolution are, therefore, felt at the exhaust nozzle, so that, for a locomotive speed between 7 and 13 km/h, a crankshaft speed between 2.8 and 4.7 Hz results, and a first-order pulse frequency, or a *piston excitation frequency*  $f_p$ , between 11 and 19 Hz is produced. The relationship between the fundamental frequency of the piston excitation and the locomotive speed,  $S$ , is therefore

$$f_p = 1.433S. \quad (1)$$

Excitation at the higher harmonics of the fundamental piston frequency is also possible, as is normally the case in piston machine applications. At 14 km/h, the fundamental piston frequency is  $f_p \approx 20$  Hz.

The intensity of the pulses depends on the tractive effort of the locomotive. For a heavy train and/or a steep gradient, the operator will set the valve gear such that fresh steam is admitted over a long portion of the piston stroke (24), so that the expansion rate is small and the steam exhausts with a still considerable pressure into the exhaust nozzle. Thus, the pressure pulsation generated by the cylinder exhaust becomes stronger as the gradient gets steeper.

The tests carried out to investigate the noise problem included measurements of pressure pulsations at the following locations (see Figure 1):  $P_1$ , inside the exhaust chamber, where the steam is exhausted from the cylinders;  $P_2$ , inside the combustion chamber;  $P_3$ , inside the atomization steam pipe leading to the burners, but upstream of its superheater (only during the first set of measurements);  $P_4$ , inside the Helmholtz resonator (only during the second

†The numbers in parentheses refer to the item number given in Figure 1.

set of measurements). In addition to the pressure pulsations, the noise level inside the driver's cabin and the vibration of the combustion chamber wall were measured.

The pressure pulsations were measured by means of Kistler pressure transducers, type 7261. A Brüel & Kjaer sound pressure meter, type 2230, was used to measure the noise level. The vibration was measured with the aid of Brüel & Kjaer accelerometers, type 4370. All signals were recorded on an eight-channel digital recorder, type Heim E8. These signals were analysed later on in the laboratory by means of a four-channel frequency analyser, type Hewlett Packard 35670A.

In order to minimize the influence of wall vibration on the measurement of pressure pulsation, the pressure transducers were connected to the pressure taps by means of short rubber hoses 10 cm in length. These hoses did not affect the accuracy of pressure measurements because their length is very small compared to the wavelength of acoustic pulsation.

The measurements were taken over many speed ramps, from *circa* 8 to 15 km/h. Attention was focused on the measurements carried out over steep slopes (25%) to ensure capturing of the strongest vibration during the tests. A certain degree of data scatter had to be accepted, because it was impossible to repeat tests at the same speed, acceleration, slope and boiler pressure.

### 3. RESULTS OF THE ORIGINAL LOCOMOTIVE

Before the initiation of this investigation, the locomotive and burner manufacturers have tried to solve the problem by altering the geometry of the fresh air inlets at the burners. This approach was followed because loud noise was generated also when the locomotive was stationary (i.e. without the excitation of the steam cylinders), suggesting that the oscillation is excited by flame instability. After several *ad hoc* measures involving changes in the swirl angle, primary and secondary air inlets and the distribution of the inlet holes, it was possible to reduce the noise level at stationary conditions to an acceptable value, but the problem remained acute at high speeds. It was therefore decided to investigate the problem in a more systematic manner, to identify the nature of the excitation mechanism and develop suitable countermeasures. The first step was a detailed measurement of the system behaviour as a function of the operating conditions. Three different processes may contribute to the excitation mechanism: (a) combustion instabilities; (b) pulsations caused by the steam exhaust at the piston frequency; and (c) pulsations in the pipe conveying the atomization steam to the burner.

Figure 2 shows typical spectra of the original locomotive (with the modified fresh air inlets) when it was travelling at 14 km/h. The pressure pulsations in the combustion and the exhaust chambers [spectra (a) and (b), respectively] are predominantly at the fundamental piston frequency ( $f_p = 20.5$  Hz) and its first harmonic ( $2f_p = 41$  Hz). These pressure pulsations are the source of the loud noise as can be seen from the noise spectrum taken inside the driver's cabin, spectrum (c). Pressure measurements in the pipe which supplies the burners with atomization steam, spectrum (d), did not show any pulsations at the noise frequency, and therefore the atomization steam does not seem to play any role in the excitation process.

It is interesting to note that the  $f_p$  and  $2f_p$ -components of the pressure pulsations inside the combustion conduits [spectra (a) and (b)] have more or less similar amplitudes, but the  $2f_p$ -component is 20 dB higher in the noise spectra measured outside, i.e. in the driver's cabin. This indicates the existence of a structural resonance mode with a frequency close to 41 Hz.

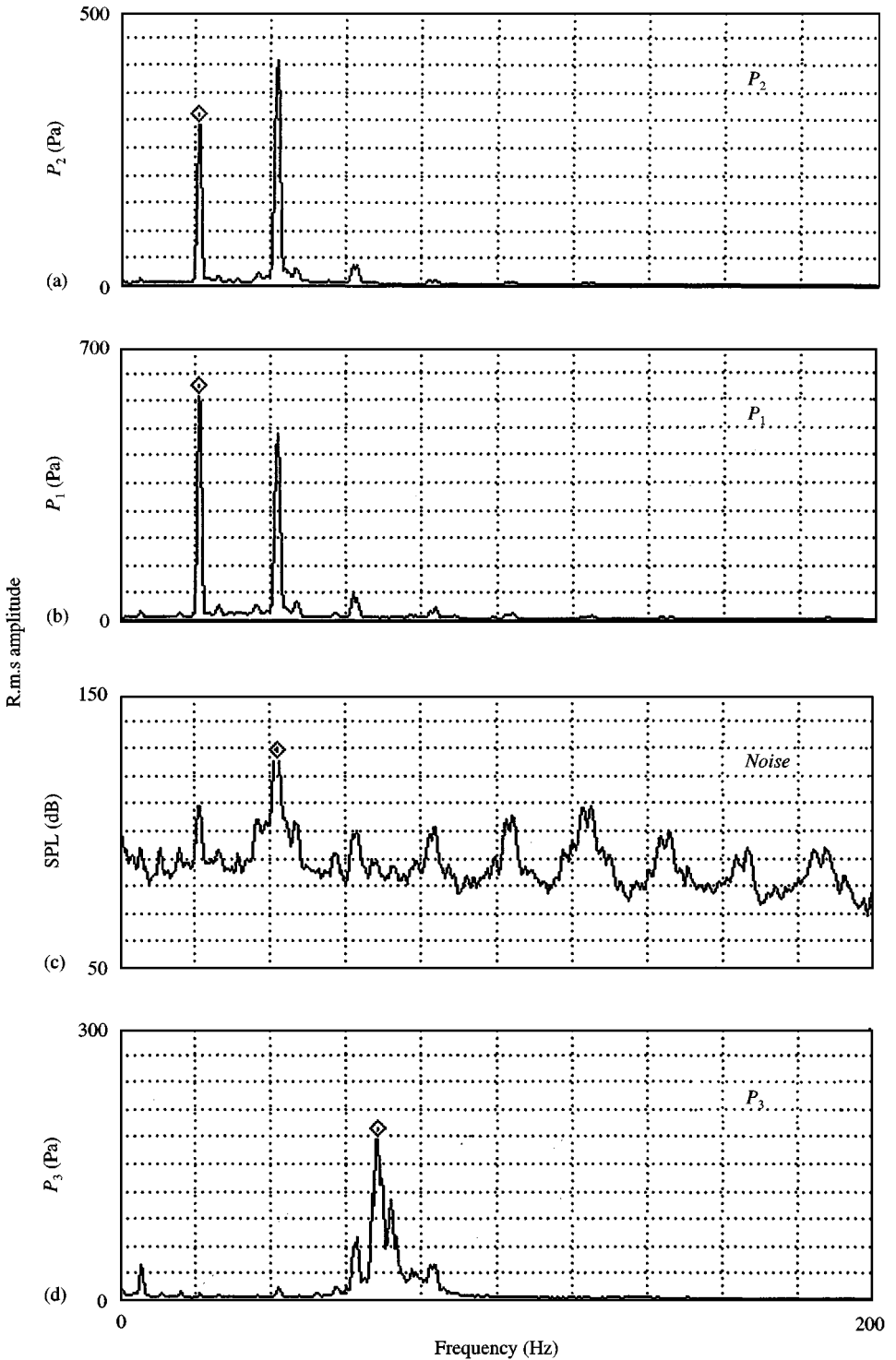


Figure 2. Typical spectra of pressure pulsations inside the combustion chamber ( $P_2$ ), the exhaust chamber ( $P_1$ ) and the atomization steam pipe ( $P_3$ ). (c) shows a noise spectrum inside the driver's cabin (in dB scale), speed:  $\approx 14$  km/h.

The severeness of the noise problem will become more apparent to the reader by a scrutiny of the noise spectrum in Figure 2. The  $2f_p$ -peak reaches 130 dB and the total sound pressure level (SPL) inside the driver's cabin exceeds 107 dB(A). This high level was reached although the microphone signal was far into the saturation range.

The effect of the locomotive speed on the pressure pulsations inside the combustion chamber and the exhaust chamber is illustrated in Figures 3–5. The spectra given in Figure 3, which correspond to several locomotive speeds, show that the pulsations occur always at the piston frequency ( $f_p$ ) and its higher harmonics. This fact is delineated in Figure 4, which compares the measured frequencies of pulsation with the piston frequency calculated from the speed, equation (1). The deviation of the data from the calculated value is within the experimental error in measuring the instantaneous speed.

The amplitudes of pressure pulsations occurring at the piston frequency  $f_p$  and its first harmonic  $2f_p$  are plotted in Figure 5 as functions of the locomotive speed. The amplitude

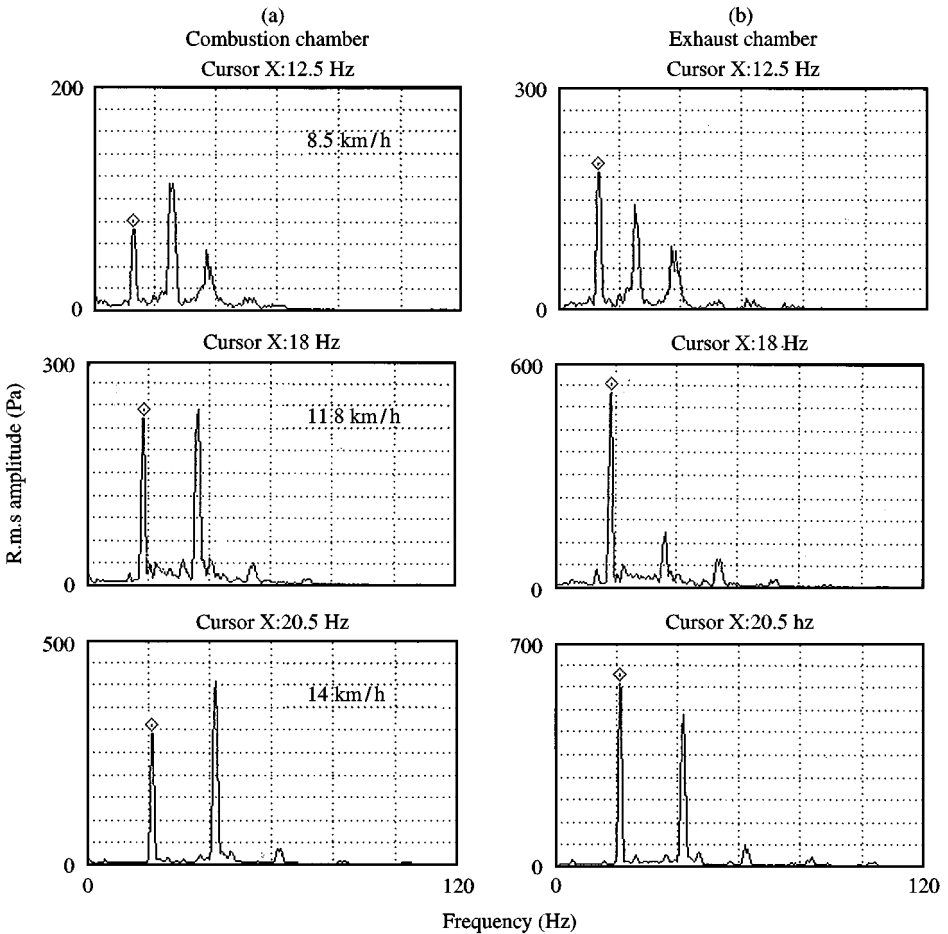


Figure 3. Effect of locomotive speed on the spectra of pressure pulsations inside (a) the combustion chamber and (b) the exhaust chamber.

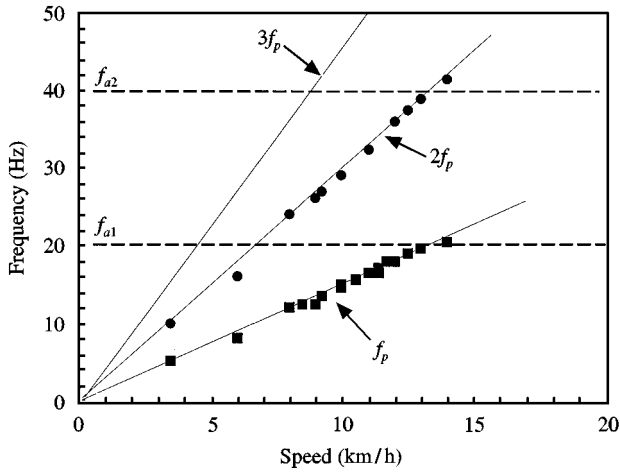


Figure 4. Main frequencies of pressure pulsations as functions of locomotive speed. The lines show the piston frequency  $f_p$ , equation (1), and its harmonics.

displays resonance characteristics; it increases rapidly when the speed is increased beyond  $\approx 11$  km/h.

#### 4. EFFECT OF FLAME INSTABILITY

It is well known that acoustic pulsations can couple and then be enhanced by flame instabilities (Rayleigh 1945; Feldman 1968; Culick 1988; Hersh 1989; among others). Under favourable conditions, a flame instability can couple with an acoustical mode of the combustion conduit and produce strong combustion oscillations. This coupling mechanism becomes self-sustaining, resulting in large amplitude pulsations, if the ‘‘Rayleigh index’’ (Rayleigh, 1945) is positive. This index is given by

$$G = \iint_{x,T} Q(x,t)P(x,t) dx dt, \quad (2)$$

where  $Q(x,t)$  is the unsteady heat release,  $P(x,t)$  represents the unsteady pressure,  $x$  is the location, and  $T$  stands for the time of one oscillation cycle. The above condition means that a favourable phase between  $P$  and  $Q$  must be maintained over the whole oscillation cycle.

In recent years [see the reviews by McManus *et al.* (1991) and Schadow *et al.* (1992)], several authors have used active control techniques to eliminate combustion oscillations by, for example, actively cancelling the effect of the acoustic field on the flame at the burner’s head (Ziada & Graf 1997). For the present problem, however, this technique was considered unsuitable because of the hazardous environment inside the combustion conduits.

As mentioned earlier, initial tests before altering the air inlets indicated that the noise problem was also encountered when the locomotive was stationary. In order to evaluate these observations and thereby clarify the role of flame instability in the excitation mechanism, additional tests were carried out whilst the locomotive was stationary (to eliminate the piston excitation altogether). In general, it was rather difficult to produce combustion oscillations when the locomotive was stationary, but for a selective

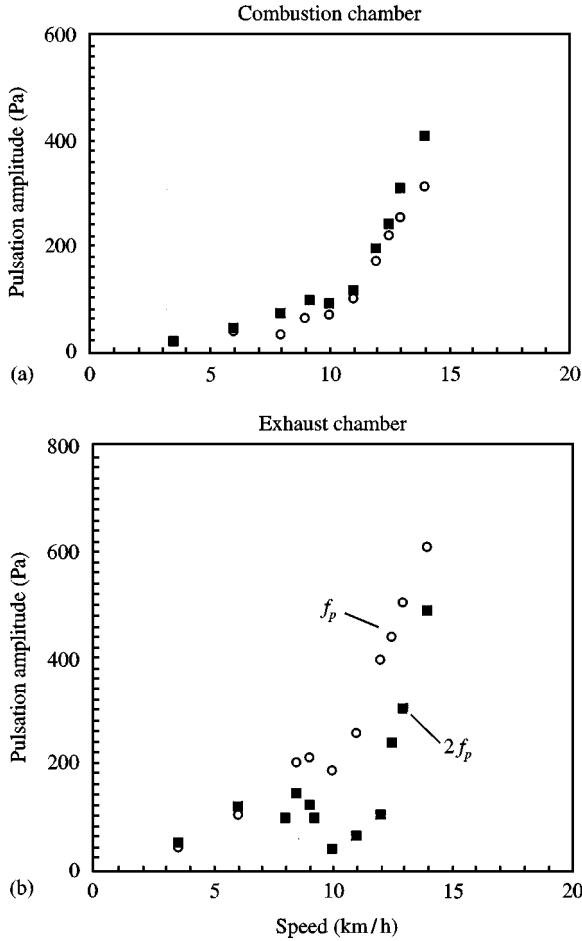


Figure 5. Amplitude (r.m.s.) of the pressure pulsations inside (a) the combustion chamber and (b) the exhaust chamber as functions of the locomotive speed. o, pressure pulsation at  $f_p$ ; ■, pressure pulsation at  $2f_p$ .

combination of flow rates of the fuel, the combustion air, and the atomization stream, oscillation did occur in the absence of the cylinder excitation. Typical pressure and noise spectra at this condition are shown in Figure 6. The occurrence of these oscillations (at  $f \approx 40$  Hz) indicates the following: (i) the combustion process is liable to acoustic excitation and therefore it can enhance pressure pulsations once they exceed a certain limit which is needed to trigger the flame instability; (ii) there is an acoustical resonance mode at approximately 40 Hz; (iii) the acoustic pulsations which will be most enhanced by the flame are those at frequencies close to approximately 40 Hz.

The last supposition explains why in the combustion chamber, the second harmonic ( $2f_p = 41$  Hz) is stronger than the fundamental component [see Figure 2(a)].

## 5. EXCITATION MECHANISM

There is no doubt that the excitation source is the pressure pulsation caused by the steam exhausting from the cylinders at the piston frequency and its harmonics: the measured

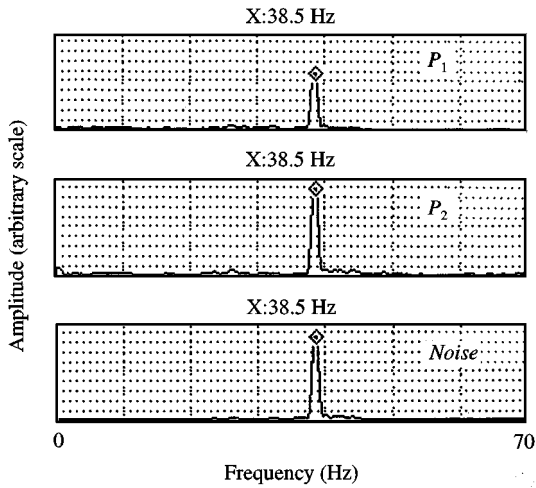


Figure 6. Typical pressure and noise spectra showing characteristics of self-excited combustion oscillations while the locomotive was stationary, i.e. without piston excitation.

pulsation frequencies increase linearly with the speed and are identical to the piston frequency and its harmonics. Preliminary analysis, in which the combustion conduits were modelled as a system consisting of two masses (heat exchanger flue and chimney) and two springs (combustion and exhaust chambers), indicated the existence of two acoustical resonance modes near the frequencies  $f_{a1} \approx 20$  Hz and  $f_{a2} \approx 40$  Hz. These are indicated in Figure 4 by the broken lines. When the piston frequencies  $f_p$  and  $2f_p$  approach these acoustic resonance frequencies, the pressure pulsation increases rapidly as can be seen in Figure 5. When the pulsation amplitude becomes sufficiently large, it excites the combustion instability which, in turn, reinforces the acoustic pulsation. The existence of two resonance modes with a frequency ratio of about 2 is rather unfortunate, because they match simultaneously the fundamental frequency of the piston excitation and its first harmonic. The excitation mechanism therefore can be classified as a resonant, forced oscillation with a reinforcement effect from the flame instability.

The excitation of the flame instability near the condition of frequency coincidence (i.e. at 13–14 km/h) is certain because the flame changes its character entirely. As observed from the glass window, it changes from a yellow/red long flame to a light blue very short flame (due to better mixing and more efficient combustion). Similar characteristics were observed when the flame instability occurred at stationary conditions, i.e. without the piston excitation.

It is helpful to have another look at the results of pressure measurements in the light of the described excitation mechanism. The pulsation amplitude curves shown in Figure 5 show a resonance response when the speed exceeds 12 km/h because the piston frequency ( $f_p > 17$  Hz) becomes close to the first-mode frequency at 20 Hz (Figure 4). At frequency coincidence, 13–14 km/h, the harmonic component  $2f_p$  becomes substantially stronger in the combustion chamber, as seen in Figure 5, because the combustion process seems to enhance pulsations near 40 Hz. In the exhaust chamber, however, the fundamental component is always stronger than the harmonic component. Another feature that can be observed in Figure 5 is the existence of a weak resonant response centred at 8.5 km/h. This seems to be



caused by a coincidence between the component  $3f_p$  and the second acoustic mode  $f_{a2}$ . This frequency coincidence can be seen in Figure 4, and the enhancement in the  $3f_p$  component at 8.5 km/h is illustrated in the top spectra of Figure 3.

## 6. ACOUSTICAL MODEL

In order to alleviate the above-described excitation mechanism, the acoustic resonance frequencies should be separated from the piston frequency over the whole range of locomotive speeds. If this is not possible, sufficient damping should be added to the system to reduce the pulsation amplitude at resonance such that it does not excite the flame instability. An additional measure which may reduce the oscillation amplitude for this particular problem, is to alter the frequencies of the first two modes such that their frequency ratio is not close to 2 (i.e.,  $f_{a2} \neq 2f_{a1}$ ).

Initially, several approaches to solve this problem were evaluated. Altering the transmission ratio to avoid frequency coincidence was out of the question because it would interfere with other optimization goals such as locomotive weight, efficiency and the driving mechanism dynamics. Silencers are not efficient at these low frequencies, and increasing damping by means of flow resistance would hinder the flow of flue gases through the system. Active control techniques were also considered to stabilize the flame or cancel the piston excitation. This approach was also considered impractical because of the harsh environment, the lowness of the frequency, in addition to the fact that stabilization of the flame would reduce the enhancement by the combustion process, but not eliminate the resonance mechanism itself which is caused by the piston exhaust. Attention was then focused on simple modifications of the combustion conduits to change the resonance frequencies and/or increase their damping.

In order to evaluate the latter approach systematically and more accurately, an acoustical model of the combustion conduits, excluding the effect of the combustion process, was developed. This model was then converted into an analogous electrical system and analysed utilizing the electrical circuits code *Pspice* (1996). By means of this method, it was possible to investigate the effect of any geometrical change on the amplitude and frequency response of the combustion conduits.

The physical model of the combustion conduits with relevant system parameters are shown schematically in Figure 7(a). Here, the chimney, the heat exchanger flue and the inlet air ducts are modelled as lumped masses to represent the inertance of the model. The combustion and exhaust chambers connecting these masses are modelled as lumped volumes and they represent the compliance of the model. The lumped model parameters are obtained by using the local fluid properties (such as the density and the speed of sound) calculated from the design data of the locomotive at full load.

The analogous electrical circuit corresponding to the acoustical model presented above is shown in Figure 8. This circuit is obtained by replacing the inertance, compliance and viscous losses of the acoustical model with the electrical parameters inductance ( $L$ ), capacitance ( $C$ ) and resistance ( $R$ ). The values of these electrical parameters are calculated from the following relations:

$$\text{Inductance: } L = \rho l_e / A, \quad (3)$$

$$\text{Capacitance: } C = V / (\rho c^2), \quad (4)$$

$$\text{Resistance: } R = 2\pi\rho f^2 / c, \quad (5)$$

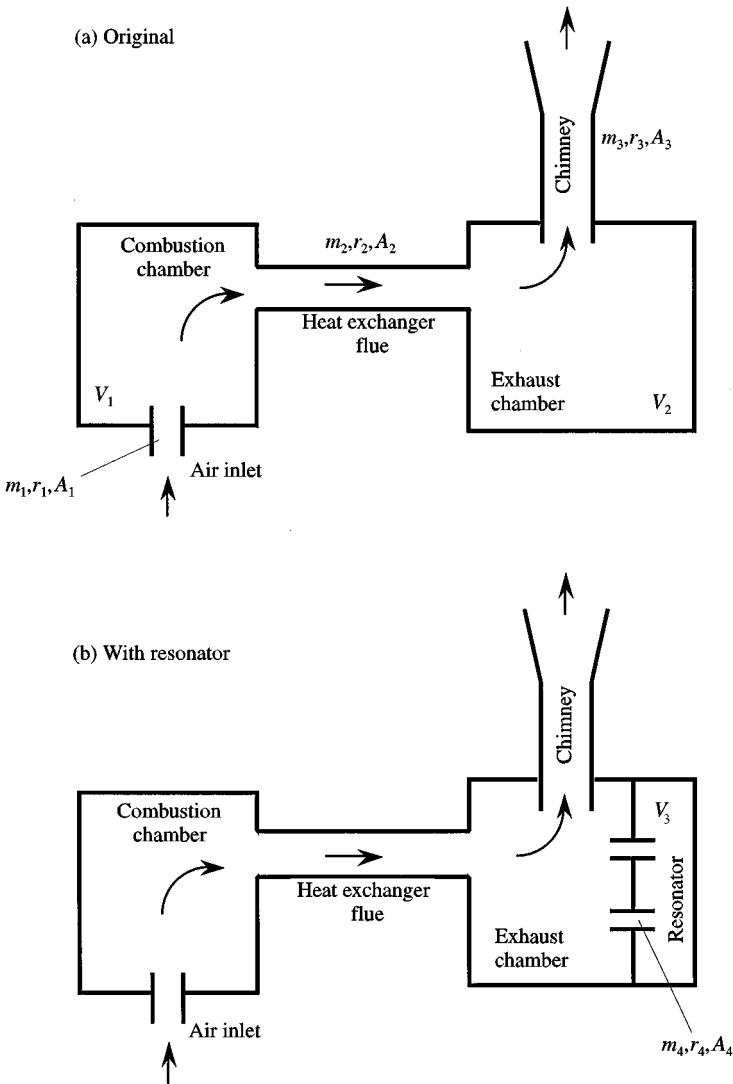


Figure 7. Simplified model of the combustion conduits (a) without and (b) with the resonator.

where  $\rho$  and  $c$  are the local density and the speed of sound of the fluid, respectively, and  $f$  is the frequency of acoustic waves;  $V$  is the associated volume (of combustion or exhaust chambers);  $A$  and  $l_e$  are the associated area and effective length (of the chimney, heat exchanger flue or inlet air ducts), respectively. Similarly, electrical analogues of the acoustical velocity and pressure are alternating current and voltage across the circuit, respectively. In Figure 8, an alternating voltage,  $V_s$ , is applied to the circuit to simulate a pressure source existing at the corresponding location in the conduits (the exhaust chamber). A more detailed discussion of this analogy is given in Kinsler *et al.* (1982) and Morse (1981).

Equation (5) given above to estimate the resistance is in an ideal form and is valid for simple pipes without flow. The actual values of the acoustic losses in the conduits of this study are expected to deviate significantly from those obtained by this relation considering

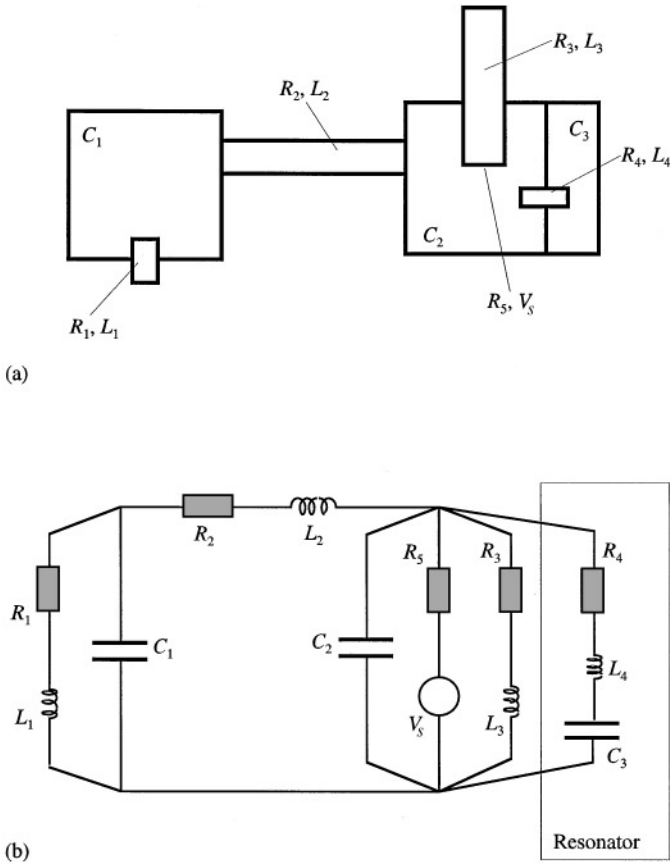


Figure 8. Electrical circuits analogous to the acoustic models shown in Figure 7. (a) without and (b) with the resonator.

their relatively complicated geometries and flow conditions. In this study, the resistance of each passage is assumed to be constant with a value estimated by means of equation (5) around an average frequency of  $f_{av} = (f_{a1} + f_{a2})/2$ . For the Helmholtz resonator, the resistance ( $R_4$  in Figure 8) calculated by equation (5) was corrected considering that the neck was filled with a damping material. According to the data given in the literature for similar material [see, e.g., Beranek (1993)], a value of  $73 \text{ kg/m}^4 \text{ s}$  was taken in the present case. The other numerical values used in the model are listed in Table 1.

It should be noted here that the objective of this simple model is not to study the whole excitation mechanism including the effect of combustion (which is a very complex task), but rather to study the effect of design changes on the frequencies of the acoustical modes.

Figure 9 shows the model frequency response to a pressure source whose frequency varies from 0 to 100 Hz. The source was positioned at the chimney inlet to simulate the excitation by the steam discharge from the cylinder (see source  $V_s$  in Figure 8). As expected, two resonance modes with frequencies of 21 and 40 Hz are predicted. In the combustion chamber, the amplitude of the first mode is stronger than the second, which contradicts the experimental data shown in Figure 2(a). This is because the combustion process is not included in the model. As mentioned earlier, the oscillations most enhanced by the flame instability are those occurring at frequencies near 40 Hz.

TABLE 1  
Numerical values used to calculate the inductance, capacitance and resistance of different components

	$\rho$ (kg/m <sup>3</sup> )	$l_e$ (m)	$A$ (m <sup>2</sup> )	$V$ (m <sup>3</sup> )	$c$ (m/s)
Inlet air ducts	1.15	0.62	0.144		348
Combustion chamber	0.229			1.512	782
Heat exchanger flue	0.304	2.92	0.138		679
Exhaust chamber	0.45			0.585*	557
Chimney	0.45	1.85	0.067		557
Resonator	0.45	0.135	0.006	0.15	557

\*This value reduces to 0.435 m<sup>3</sup> after installing the resonator.

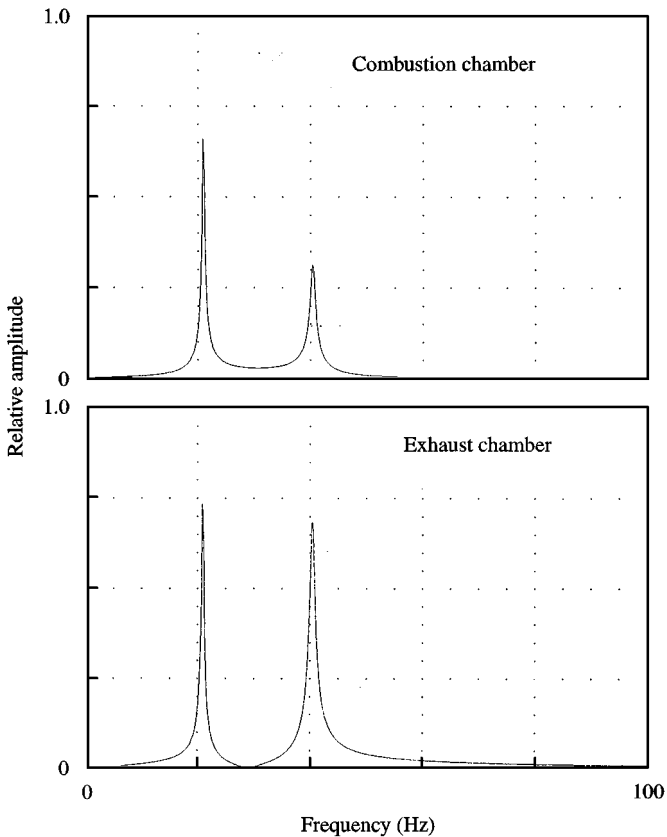


Figure 9. Simulation results showing the frequency response of the original system to a pressure source located at the inlet of the chimney.

The effect of several geometrical changes on the system acoustic response was then studied by means of the electrical model. Simple design changes, such as reducing the volume of the combustion or the exhaust chambers [the term  $V$  in equation (4)] within the allowable limits, did not increase the frequency of the first mode sufficiently to avoid

coincidence with the piston frequency. The second-mode frequency, however, could be increased by reducing the volume of the exhaust chamber. Since changes in the mechanical transmission ratio were out of the question, coincidence between the piston frequency  $f_p$  and the first acoustic mode  $f_{a1}$  could not be avoided.

The possibility of adding a Helmholtz resonator inside the exhaust chamber seemed to be the most practical and simple approach. Space for the resonator was available in the exhaust chamber and the resulting reduction in the volume of this chamber can sufficiently increase the frequency of the *second acoustic mode* beyond the piston excitation at  $2f_p$ . Additionally, the resonator can be tuned to the *first acoustic mode* and a flow resistance can be added in its neck to increase the frequency range of amplitude attenuation. Thus, a resonator with the maximum possible volume and with four necks was designed and tested by means of the developed model. Initially, the necks were chosen to match the first acoustic mode ( $f_{a1} = 21$  Hz) and were presumed to be filled with steel wool to increase the damping. The geometry was then optimized to maximize the attenuation of the first acoustic mode. The physical model including the Helmholtz resonator is shown in Figure 7(b), see also Figure 1, and the analogous electrical circuit including the analogue of the added Helmholtz resonator is shown in Figure 8.

The response of the acoustic model with the final resonator geometry is illustrated in Figure 10. The amplitude of the first mode ( $f_{a1}$ ) is seen to be strongly reduced in the

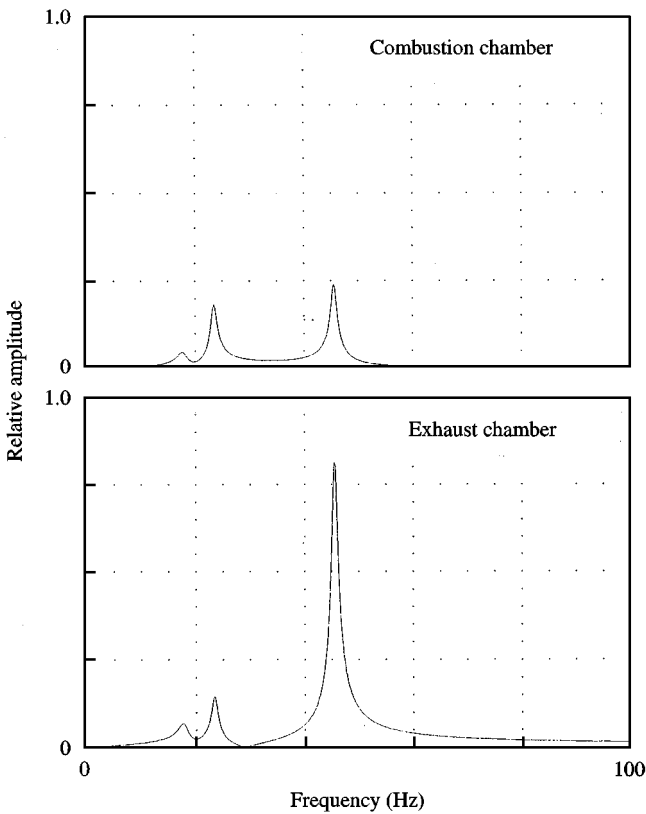


Figure 10. Simulation results showing the frequency response of the system with the resonator to a pressure source located at the inlet of the chimney.

combustion and exhaust chambers. In addition, the frequency of the second mode ( $f_{a2}$ ) is increased to 46 Hz, which is sufficiently higher than the second harmonic of the piston frequency at 14 km/h ( $2f_p = 40$  Hz).

The above results were obtained by using a resonator with a volume of  $0.15\text{ m}^3$  (which is 36% of the original exhaust chamber volume) and with four necks (“in parallel”), each 44 mm in diameter and 152 mm in length. A resonator with this geometry was then manufactured and installed in the locomotive.

### 7. RESULTS OF THE LOCOMOTIVE WITH RESONATOR

Figures 11 and 12 show typical pressure and noise spectra of the locomotive with and without the resonator, respectively. All spectra were taken at a speed of approximately 14 km/h and on the same slope to ensure that the excitation energy by the cylinder exhaust is similar in both cases. When the resonator is installed, the pressure pulsation inside the exhaust chamber ( $P_1$ ) is smaller by a factor of 17 dB and that inside the combustion chamber is reduced by 12 dB. The noise spectra inside the driver’s cabin show a similar trend; the spectral peak is reduced by an amount of 12 dB.

The above-mentioned reductions in the pressure pulsations and the noise level become even more substantial when the total r.m.s. amplitude is considered. This is illustrated in Figure 13 which shows the total sound pressure level (SPL) inside the driver’s cabin as a function of the locomotive speed. A reduction of 21 dB(A) is achieved at 14 km/h. In fact, the actual amount of noise reduction is higher than 21 dB(A), because the microphone signal at 14 km/h was saturated (or overloaded) during the measurement without the resonator.

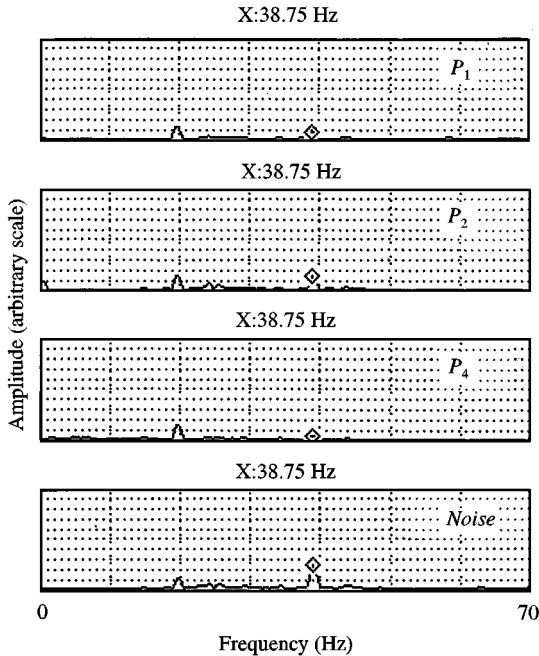


Figure 11. Pressure and noise spectra of the locomotive with the resonator, speed  $\approx 14$  km/h.

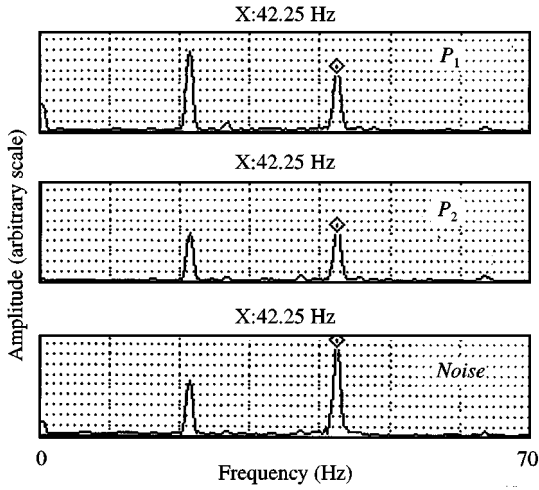


Figure 12. Pressure and noise spectra of the locomotive without the resonator. Locomotive speed  $\approx 14$  km/h.

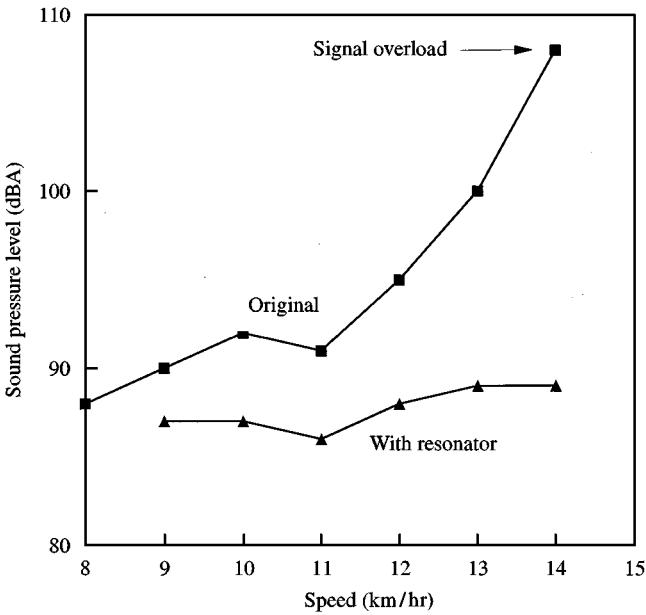


Figure 13. Sound pressure level (SPL) inside the driver’s cabin as a function of the locomotive speed; ■, without the resonator; ▲, with the resonator.

### 8. CONCLUSIONS

The pressure pulsations inside, and the noise emitted by a steam locomotive have been measured to clarify the cause of the loud noise generated when the locomotive speed exceeds the design value. The acoustic resonance modes of the combustion conduits are

found to be excited by the pressure pulsations produced by the steam exhaust from the cylinders. When these resonances are initiated, the acoustic pulsations excite the flame instabilities which, in turn, enhance the resonance. The resonance was particularly strong because the piston frequency and its second harmonic coincided with the first- and second-mode frequencies, simultaneously.

An acoustical model of the combustion conduits has been created and then used to design a Helmholtz resonator with the objectives of dampening the response of the first acoustic mode and shifting the frequency of the second mode, such that frequency coincidence with the second mode is avoided. The neck of the resonator was filled with steel wool to increase the system damping near the first-mode frequency. The installation of the resonator reduced the pressure pulsation inside the locomotive by an amount up to 12 dB, and the noise level inside the driver's cabin by an amount exceeding 21 dB(A).

#### REFERENCES

- BERANEK, L. L. 1993 *Acoustics* Woodburg, NY: Acoustical Society of America.
- CULICK, F. E. C. 1988 Combustion instabilities in liquid-fuelled propulsion systems—An overview. *AGARD 72B PEP Meeting*, Bath, England.
- FELDMAN, K. T. 1968 Review of the literature on sondhauss thermoacoustic phenomena. *Journal of Sound and Vibration* **7**, 83–89.
- HERSH, A. S. (ed.) 1989 *Proceedings of Symposium on Combustion Instabilities Driven by Thermo-Chemical Acoustic Sources*. ASME Publication No. NCA - 4, Vol. HTD - 128.
- KINSLER, L. E., FREY, A. R., COPPENS, A. B. & SANDERS, J. V. 1982 *Fundamentals of Acoustics*, 3rd edition. New York: J Wiley.
- MORSE, P. M. 1981 *Vibration and Sound*, Paperback edition. Woodburg, NY: American Institute of Physics.
- MCMANUS, K. R., POINSET, T. & CANDEL, S. M. 1991 A review of active control of combustion instabilities. *Proceedings International Symposium on Pulsating Combustion*, Monterey, Calif., U.S.A.
- Pspice* 1996 A computer code to simulate electrical circuits. Micro-Sim Corporation, Irvine, CA, Version 6.3.
- RAYLEIGH, LORD 1945 *The Theory of Sound*, Vol. 2, p. 227. New York: Dover.
- SCHADOW, K. C., HENDRICKS, E. W. & HANSEN, R. J. 1992 Recent progress in the implementation of active combustion control. *Proceedings 18th Congress International Council of the Aeronautical Sciences*, Beijing, China.
- ZIADA, S. & GRAF, H. R. 1997 Feedback control of combustion oscillations. *Proceedings 4th International Symposium on Flow-Induced Vibration and Noise* (eds M. P. Paidoussis et al.), ASME International Mechanical Engineering Congress & Exposition, November 1997, Dallas, TX, U.S.A., Vol. II, pp. 329–338. New York: ASME. Also *Journal of Fluids and Structures* **12**, 491–507.

#### APPENDIX: NOMENCLATURE

$A$	cross sectional area
$d$	diameter
$f$	frequency
$f_{a1}, f_{a2}$	frequencies of the first and second acoustic modes
$f_p$	fundamental piston frequency
$c$	local speed of sound in fluid
$C$	analogous electrical capacitance
$l$	tube length
$l_e$	effective length, $l + 0.85d$
$L$	analogous electrical inductance
$m$	mass ( $= \rho l_e A$ )



$r$	acoustic resistance
$R$	analogous electrical resistance
$S$	locomotive speed
$V$	volume
$V_s$	alternating voltage representing the excitation by the steam cylinders
$\rho$	density of fluid

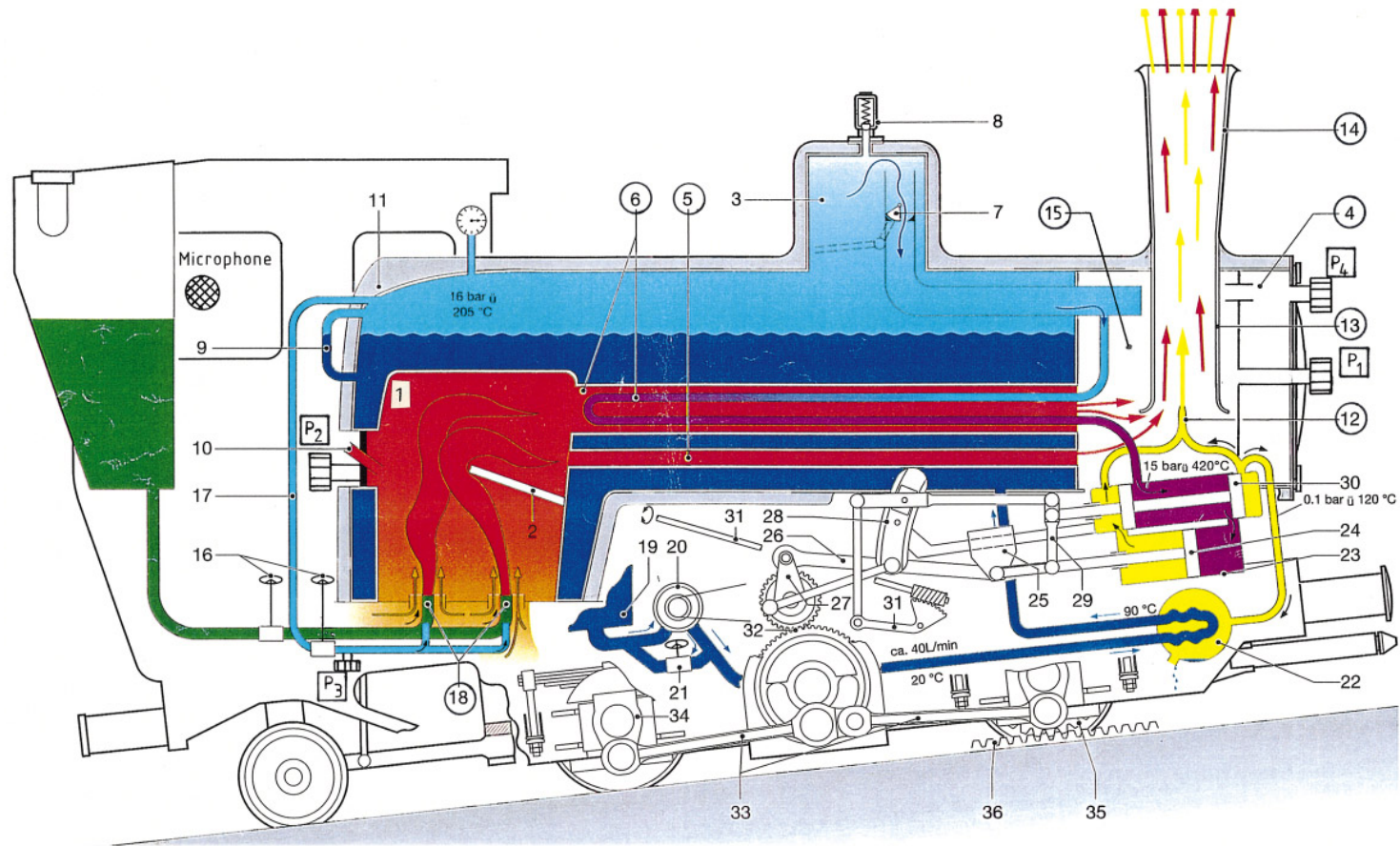


Figure 1. Geometry of the locomotive and locations of pressure measurements. 1: combustion chamber; 4: resonator; 5 and 6: heat exchanger flue; 12: exhaust steam nozzle; 13 and 14: chimney; 15: exhaust chamber; 18: burner.